

# Aligning Foundation Model Priors and Diffusion-Based Hand Interactions for Occlusion-Resistant Two-Hand Reconstruction

Gaoge Han

Yongkang Cheng

Zhe Chen

Shaoli Huang

Tongliang Liu

## Abstract

*Two-hand reconstruction from monocular images faces persistent challenges due to complex and dynamic hand postures and occlusions, causing significant difficulty in achieving plausible interaction alignment. Existing approaches struggle with such alignment issues, often resulting in misalignment and penetration artifacts. To tackle this, we propose a novel framework that attempts to precisely align hand poses and interactions by synergistically integrating foundation model-driven 2D priors with diffusion-based interaction refinement for occlusion-resistant two-hand reconstruction. First, we introduce a Fusion Alignment Encoder that learns to align fused multimodal priors — keypoints, segmentation maps, and depth cues from foundation models — during training. This provides robust structured guidance, further enabling efficient inference without foundation models at test time while maintaining high reconstruction accuracy. Second, we employ a two-hand diffusion model explicitly trained to transform interpenetrated poses into plausible, non-penetrated interactions, leveraging gradient-guided denoising to correct artifacts and ensure realistic spatial relations. Extensive evaluations demonstrate that our method achieves state-of-the-art performance on InterHand2.6M, FreiHAND, and HIC datasets, significantly advancing occlusion handling and interaction robustness. Our code will be publicly released.*

## 1. Introduction

3D two-hand recovery aims to reconstruct both hands of a person in 3D space, a crucial task for numerous emerging applications, including 3D character animation, augmented and virtual reality (AR/VR), and robotics. Large-scale hand datasets [13, 14] have greatly facilitated numerous studies on hand recovery. These approaches can be summarized as focusing on scaling up datasets [17], improving backbone [9, 17], and incorporating attention mechanisms [7, 8, 25] between the hands.

Recent advancements in the related area have highlighted the benefits of foundation model priors and genera-

tive priors in improving 3D reconstruction tasks. For example, in the task of 3D human recovery, WHAM [20] utilizes 2D human keypoint model to extract motion features as priors. TRAM [23] further employs segmentation maps and depth maps to help to regress the kinematic body motion of a human. BUDDI [15] reconstructs two individuals in close proximity by utilizing the diffusion model as a prior. These show that vision foundation model-inferred structured 2D cues, e.g. keypoint, segmentation mask, and depth, provide valuable prior knowledge for 3D hand reconstruction. However, a challenging issue persists: the misalignment between 2D foundation model priors and 3D hand representations. Directly applying or finetuning 2D information features with foundation models would be non-trivial in transforming them seamlessly into accurate 3D hand structures, as 2D-3D feature alignment is inherently ambiguous. Beyond this misalignment, 3D reconstruction introduces an additional challenge: interaction consistency. In occlusion scenarios, one hand may block key regions of the other in 2D space, making it difficult to infer plausible inter-hand interactions. Existing methods, especially hand reconstruction approaches [8, 12, 25], would still suffer from spatial inconsistencies, unnatural interactions, and interpenetration artifacts due to potentially weakly constrained interaction priors.

To overcome the above alignment issues, we propose a unified framework that integrates foundation model-driven 2D priors with diffusion-based interaction refinement. We progressively utilize these two to enhance the alignment performance from 2D to 3D spaces for occlusion-resistant two-hand reconstruction. Firstly, we leverage the exceptional performance of foundational models in 2D vision tasks and use them to generate 2D keypoints, segmentation maps, and depth maps as strong priors for providing well-structured 2D reference guidance. 2D keypoints provide accurate spatial information about hand joints in the image plane, segmentation maps offer a detailed prior of hand shapes and boundaries, and depth maps encode pixel-level depth cues that better capture the hands' relative positioning in 3D space. We then introduce a Fusion Alignment Encoder that learns to align key points, segmentation, and depth priors from a suite of vision foundation models [5]

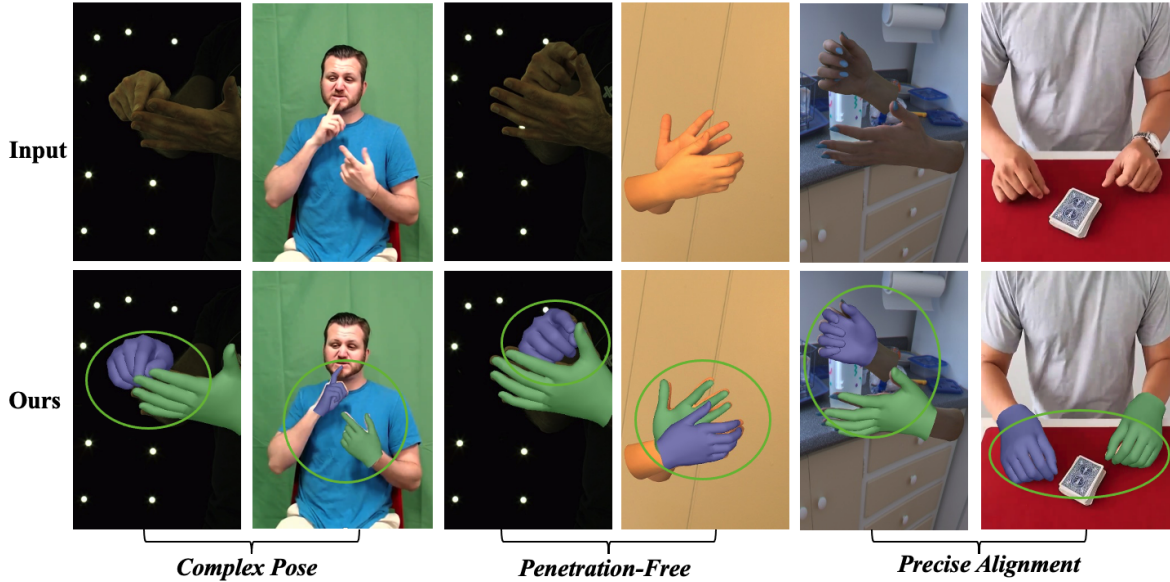


Figure 1. Two-hand recovery on InterHand2.6M (1st, 3rd rows), Re:InterHand (4th, 5th rows), and In-the-Wild (2nd, 6th rows).

during training. This encoder distills 2D prior information into the same latent feature space and aligns them together and allows us to waive the explicit use of the vision foundation model during inference. Subsequently, a hand regressor estimates hand parameters based on the fused features. Secondly, we employ a two-hand diffusion model to align and ensure interaction consistency by learning to correct interpenetration artifacts through gradient-guided denoising. Aligning with plausible interactions is particularly important in hand reconstruction since one hand could usually occlude important fingers of the other hand, leading to penetration issues in 3D space. The introduced 2D vision priors are still primarily in 2D space and would not be sufficient to deal with the occluded parts. Considering that diffusion models are exceptional at complementing missing 2D vision cues, we devise a two-hand diffusion model that explicitly incorporates the inter-hand penetration as a condition to enable direct learning of plausible interaction between hands. This would ensure spatially consistent and occlusion-aware hand reconstructions. Overall, our approach effectively aligns vision foundation model priors while simultaneously ensuring plausible hand interactions with our diffusion model, ensuring that two-hand reconstructions remain geometrically accurate and interaction-consistent, even under occlusions. As shown in Figure 1, we achieve robust hand reconstruction across various scenes and interactive poses.

Our key contributions can be summarized as follows.

- We propose the integration of supplementary 2D reference information as prior constraints and structured guid-

ance in the 2D domain for 3D hand reconstruction. Concurrently, we introduce a fusion alignment encoder designed to learn the vision foundation model at the latent feature level, thereby enabling the exemption of the vision foundational model during the inference phase.

- We train a two-hand diffusion model conditioned on the interpenetrating hands to directly model the interaction priors. We employ the two-hand generation model with penetration gradient guidance to address the penetration issue after two-hand estimation.
- Our approach achieves state-of-the-art performance across multiple datasets. Extensive ablation experiments further validate the improvements in model performance brought by the alignment of 2D priors and the diffusion-model-enhanced hand interactions. Our qualitative experiments in real-world scenarios also demonstrate superior alignment and depth recovery capabilities.

## 2. Related work

### 2.1. 3D hand recovery

With the introduction of some high-quality hand datasets, recovering 3D hand MANO [19] parameters from monocular input images has recently achieved remarkable advancements. For single-hand recovery, METRO [28] employs a convolutional neural network to extract a single global image feature and performs position encoding by repeatedly concatenating this image feature with the 3D coordinates of a mesh template. MeshGraphormer [9] introduces a graph-convolution enhanced transformer to effectively model both

local and global interactions. AMVUR [3] proposes a probabilistic approach to estimate the prior probability distribution of hand joints and vertices. Zhou et al. [29] simplifies the process by decomposing the mesh decoder into a token generator and a mesh regressor, achieving high performance and real-time efficiency through a straightforward yet effective baseline. HaMeR [17] highlights the significant impact of scaling up to large-scale training data and utilizing high-capacity deep architectures for improving the accuracy and effectiveness of hand mesh recovery. For two-hand recovery, IntagHand [7] propose a GCN-based network to reconstruct two interacting hands from a single RGB image, featuring pyramid image feature attention (PIFA) and cross hand attention (CHA) modules to address occlusion and interaction challenges. InterWild [12] bridges Mo-Cap and ITW samples for robust 3D interacting hands recovery in the wild by leveraging single-hand ITW data for 2D scale space alignment and using geometric features for appearance-invariant space. ACR [25] explicitly mitigates interdependencies between hands and between parts by leveraging center and part-based attention for feature extraction. 4DHands [8] handles both single-hand and two-hand inputs while leveraging relative hand positions using a transformer-based architecture with Relation-aware Two-Hand Tokenization (RAT) and a Spatio-temporal Interaction Reasoning (SIR) module. Although these methods have generally achieved competitive results in hand pose and shape reconstruction, their performance in finer details is still lacking.

## 2.2. Integrating additional information

Recently, many studies have attempted to introduce additional reference information as guidance in visual tasks to achieve better performance. For example, in the task of human digitization, ECON [24] takes as input an RGB image and is conditioned on the rendered front and back body normal images. This strategy allows it to excel at inferring high-fidelity 3D humans in loose clothing and challenging poses. For text-to-image generation, ControlNet [27] has also successfully utilized different types of conditional inputs, such as sketches, depth maps, and segmentation maps. It has successfully achieved the generation of images aligned with these conditional guides using a pretrained text-to-image diffusion model. For the 3D human motion estimation task, WHAM [20] uses human 2D keypoints to extract motion features as inputs for both the Motion Decoder and Trajectory Decoder. This approach achieves more robust and stable 3D human motion estimates in global coordinates. Zuo et al. [31] captured interaction priors in the latent space of a VAE and applied them to interacting hand reconstruction, effectively estimating plausible hand poses. InterHandGen [6] trained a cascaded two-hand generation model, which serves as a generative prior to formulate a loss

regularizer for addressing the challenge of two-hand reconstruction. In this paper, we attempt to acquire intermediate 2D hand information as 2D domain constraints and utilize a two-hand diffusion-based interaction prior to respectively address 2D and 3D alignment challenges in hand parameter estimation.

## 3. Method

In this Section, we present the technical details of our method. As illustrated in Fig. 2, distinguishing from previous hand estimation methods, our approach primarily involves introducing additional 2D information in training to guide the two-hand MANO [19] parameter estimation. Then, the estimated two-hand parameters are refined using a two-hand diffusion model.

### 3.1. Two-hand reconstruction model

Previous methods take a monocular image as input and utilize a backbone network to extract image features for the regression of hand MANO parameters. Given a monocular hand image, we endeavor to introduce structured information as a reference, ranging from local hand keypoints to depth cues, collectively ensuring better alignment to 3D pose and shapes.

**2D hand keypoints.** Inspired by WHAM [20], which extracts whole-body 2D keypoints to identify human features, we focus on extracting 2D hand keypoints as hand features, distinct from pixel-level features. These 2D keypoints provide precise locations of critical hand features, such as joints and fingertips, enabling a more accurate understanding of hand poses. For extracting 2D keypoint features, unlike WHAM, which employs an MLP and requires additional 2D-to-3D pretraining, our method eliminates these extra training steps and aligns them in image space, creating a more efficient framework for integrating diverse types of information.

**Two-hand segmentation map.** Segmentation maps provide pixel-level information, allowing for precise localization of the hand and its parts. They also help isolate hands from the background, reducing noise and distractions. By focusing on segmented areas, models can extract relevant hand features more effectively. It is worth noting that when there is significant interleaving of the two hands, the prediction results for the 2D keypoint pairs of the hands can be unreliable. However, the segmentation map can still provide reasonably accurate 2D contour information of the hands at this time (the hand segmentation map does not distinguish between the left and right hands when the Intersection over Union (IoU) for both hands is greater than 0).

**Hand depth map.** Depth maps provide information about the distance between the hands and the camera, helping to capture the relative positioning and spatial relationship of the hands in a real environment. Depth information is less

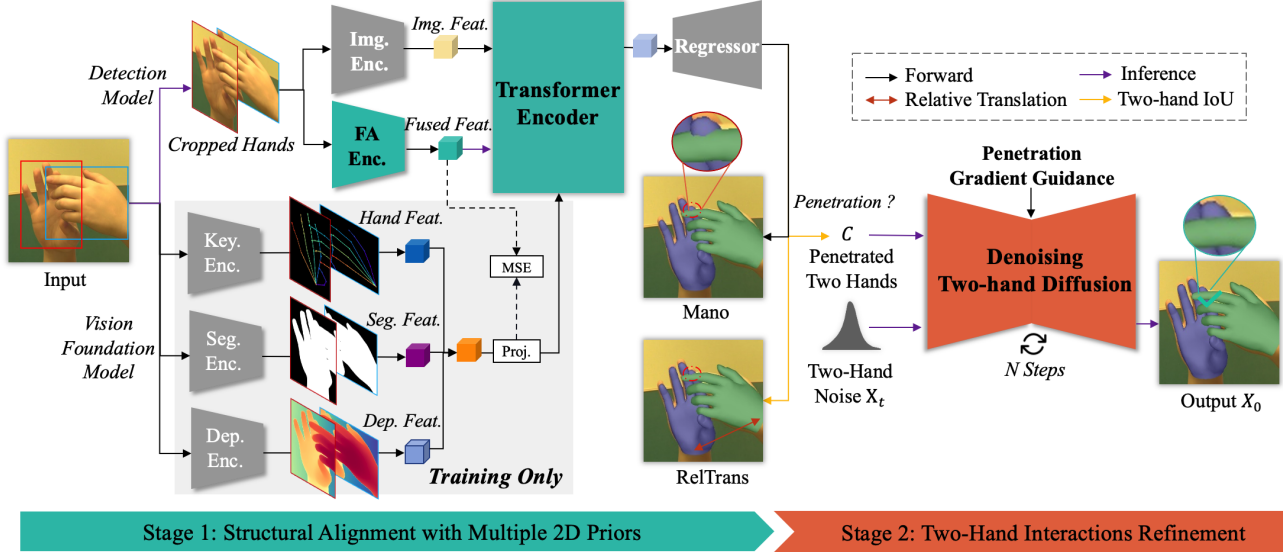


Figure 2. The overall pipeline of our proposed method. “Feat.”, “Proj.”, “Enc.”, “FA”, “Key.”, “Seg.”, “Pen.” and “RelTrans” are abbreviations for “Feature”, “Projection”, “Encoder”, “Fusion Alignment”, “Keypoints”, “Segmentation”, “Penetration” and “Relative Translation”, respectively.  $c$  denotes the condition of penetrated two hands. The purple arrow path will be activated during inference, while the yellow arrow path will be activated when the Intersection over Union (IoU) of both hands is greater than 0.

affected by variations in lighting conditions, making hand understanding more reliable in environments with varying or poor lighting.

**Fusion alignment encoder.** The process of integrating auxiliary information involves going from RGB hand images to explicit representations like keypoints, segmentation maps, and depth maps, and then to the corresponding feature embeddings. Our goal is to acquire feature embeddings of the additional information rather than these explicit outputs directly. Predicting embeddings from images is generally easier than directly predicting explicit task outputs. Therefore, we propose a fusion alignment encoder to learn the auxiliary information embeddings directly from the image by distilling the vision foundation model with MSE loss, as shown in stage 1 of Fig. 2. This approach allows us to bypass the need for additional foundation models to obtain these auxiliary features during inference.

**Multiple features fusion with transformer encoder.** We consider using a simple approach to fuse different feature information, specifically by employing a Transformer encoder. The self-attention mechanism in the Transformer encoder allows each feature token to attend to every other token in the input sequence. This enables the model to capture long-range dependencies and integrate information globally. Before aligning the foundation model priors, we aggregate and average high-level features to ensure a more consistent and semantically rich representation, aiming to reduce modality-specific biases, smooths local inconsisten-

cies, and enhances global structural coherence, leading to a more stable alignment process. Given  $F_i$ ,  $F_k$ ,  $F_m$ , and  $F_d$  to represent the input feature of hand image, 2D keypoints, segmentation map and depth map, the fused auxiliary feature  $F_a$  can be expressed as:

$$F_a = Proj((F_k + F_s + F_d)/3), \quad (1)$$

then the final integrated feature  $F$  can be expressed as:

$$F = TransEnc(\langle F_i, F_a \rangle)[0 : l], \quad (2)$$

Here,  $\langle, \rangle$  denotes the concat operation.  $TransEnc$  represents the Transformer encoder.  $Proj$  denotes the projection layer to align dimension,  $l$  denotes the image feature length. **Loss function.** The fused feature  $F$  is then input into the two-hand regressor to regress the parameters of both hands and relative translation. Building on previous two-hand recovery approaches [12, 25], We train our model in an end-to-end fashion by minimizing the L1 distance between the predicted and ground truth (GT) MANO parameters, the 3D and 2.5D joint coordinates, as well as the 3D relative translation. For training the Fusion Alignment Encoder, we use MSE loss.

### 3.2. Two-hand diffusion generation model

In addition to 2D prior alignment, we argue that the reconstructed hands may still suffer from inconsistency in physical interactions where one hand occludes the important fingers of the other hand. In this scenario, the three types of

additional information mentioned earlier are unable to provide effective guidance for the occluded parts of the hand. Consequently, the estimated occluded regions of both hands are prone to penetration issues.

To address this problem, we train a two-hand diffusion model to restore clear hand poses using corresponding penetrated reference two-hands as conditional input and incorporate penetration gradient guidance during the denoising phase. For penetrated two-hands, we generate them using two approaches: (1) the first involves synthesizing them with a low-performance two-hand estimation model and selecting the interpenetrated two-hand results. (2) the second applies slight noise to the ground truth MANO parameters of the hands until penetration occurs. Our method significantly differs from and holds advantages over InterHand-Gen [6] and zuo et al. [31], as we explicitly model a diffusion model capable of learning interactive penetration prior information. As shown in Stage 2 of Fig. 2, before using the two-hand diffusion model, we perform an IoU and penetration check between the two hands to reduce unnecessary diffusion inference in most cases. The gradient-guided two-hand diffusion effectively alleviates the penetration problem of the occluded regions.

**Loss function.** Our two-hand diffusion loss minimizes the L2 distance at each timestep between the clean hands  $X_0$  and the noisy hands  $X_t$  input to the model, conditioned on the timestep  $t$  and the penetrated hand inputs  $c$ .

**Penetration gradient guidance.** During inference, we introduce a gradient-guided strategy to resolve hand-hand occlusion and prevent interpenetration. At each denoising step of the reverse diffusion process, we compute a collision loss between both hands and iteratively adjust hand poses via gradient descent. Specifically, clean two-hand parameters  $\hat{X}_0$  are first estimated from  $X_{t-1}$  using DDIM sampling. These parameters are fed into the MANO model to obtain mesh vertices  $V_{t-1}$  and  $V_c$ . To accurately detect collisions, we design a hybrid distance-orientation criterion: 1) Calculate Chamfer distances  $N_{ij} = \|V_{t-1}^i - V_c^j\|^2$  and retain vertex pairs with  $N_{ij} < d_{\text{threshold}}$ . 2) For retained pairs, compute the cosine similarity  $\cos(\theta_{ij})$  between their normal vectors, identifying collisions when  $\cos(\theta_{ij}) < \cos(\theta_{\text{thre}})$ . This yields a collision set  $C_{\text{col}}$ . We then formulate a robust collision loss using the GMoF function:

$$L_{\text{collision}} = \sum_i \sum_j \left( \frac{\|V_{t-1}^i - V_c^j\|^2}{\|V_{t-1}^i - V_c^j\|^2 - \rho} \right), \quad (3)$$

and update  $\hat{X}_0$  by propagating the negative gradient of this loss:

$$\hat{X}_0 = \hat{X}_0 - \lambda(\delta_i L_{\text{collision}}), \quad (4)$$

where  $\lambda$  controls the adjustment magnitude.

Overall, the two-hand diffusion model refines hand interactions by iteratively denoising interpenetrated poses, grad-

ually guiding them toward physically plausible configurations. This could learn an implicit interaction prior from data, enabling it to model complex spatial relationships and enforce realistic inter-hand alignment even under severe occlusions.

## 4. Experiments

### 4.1. Implementation details

**Two-Hand Reconstruction Model.** We implement our network using PyTorch [16]. For the image feature extractor, we use ResNet-50 [2] as the backbone, while for additional 2d information encoders and fusion alignment encoder, we use Sapiens [5] and ResNet-50. The hand bounding box detector utilizes RTMDet [11]. Our model is trained on 4 A100 GPUs using the AdamW optimizer, starting with an initial learning rate of  $1e-4$ , which is reduced by a factor of 10 at the 4th epoch. We use a mini-batch size of 48. For other details, we follow the approach in [12], the left hand is flipped to align with the right-hand input to the network, and after prediction, the results are flipped back. Our training dataset only a few representative two-hand and single-hand datasets, including InterHand 2.6M [13], Re:InterHand [14], COCO whole-body [4], FreiHand [30] and HO-3D [1], which is less than the experimental setups of the latest methods 4DHands [8] (3 types of two-hand datasets and 9 types of one-hand datasets). We believe this better demonstrates the effectiveness of our proposed approach. For testing, we primarily use InterHand 2.6M, FreiHAND and the in-the-wild dataset HIC [22].

**Two-Hand Diffusion Model.** We employ a transformer-based architecture for our two-hand diffusion model, utilizing MLPs to encode the input timesteps and fully connected layers to encode the interpenetrated two-hand inputs and predict the clean two-hand outputs. The diffusion model adopts an MDM-style [21] diffusion process to enhance geometric learning. This model has been trained with 1,000 noising steps and a cosine noise schedule. The training datasets include InterHand 2.6M [13] and Re:InterHand [14].

### 4.2. Datasets

**InterHand 2.6M** [13] features both precise human (H) and machine (M) 3D pose and mesh annotations, encompassing 1.36 million frames for training and 850,000 frames for testing. **Re:InterHand** [14] consists of 739K video-based images and 493K frame-based images from third-person viewpoints, and 147K video-based images from egocentric viewpoints. **COCO WholeBody** [4] extends the COCO dataset [10] by adding comprehensive whole-body annotations. It includes manual annotations covering the entire human body. **FreiHand** [30] is a dataset designed for single-hand 3D pose estimation, providing MANO annotations for

Methods	MRRPE	MPJPE	MPVPE	IH MPJPE	IH MPVPE	SH MPJPE	SH MPVPE
Moon et al. [13]	-	13.98	-	16.02	-	12.16	-
Zhang et al. [26]	-	11.58	12.04	11.28	12.01	11.73	12.06
IntagHand [7]	-	9.95	10.29	10.27	10.53	9.67	9.91
Zuo et al. [31]	-	8.34	8.51	-	-	-	-
ACR [25]	-	8.09	8.29	9.08	9.31	6.85	7.01
InterWild [12]	26.74	7.85	8.16	8.24	8.68	6.72	6.93
Ren et.al [18]	28.98	7.51	7.72	-	-	-	-
4DHands [8]	24.58	7.49	7.72	-	-	-	-
<b>Ours</b>	<b>21.60</b>	<b>5.36</b>	<b>5.58</b>	<b>5.93</b>	<b>5.87</b>	<b>4.84</b>	<b>4.86</b>
<b>Ours*</b>	<b><u>20.82</u></b>	<b><u>5.11</u></b>	<b><u>5.35</u></b>	<b><u>5.62</u></b>	<b><u>5.58</u></b>	<b><u>4.56</u></b>	<b><u>4.59</u></b>

Table 1. Comparison with state-of-the-art methods on InterHand2.6M[13] 5fps test dataset. The results that are bolded and underlined represent the best result, while the bolded results represent the second-best result. \* indicates that we use the foundation model [5] for inference.

Methods	MRRPE	MPJPE	MPVPE
IntagHand [7]	73.04	20.38	21.56
InterWild [12]	26.43	15.62	15.17
4DHands [8]	25.26	9.32	9.93
<b>Ours</b>	<b>22.24</b>	<b>6.67</b>	<b>6.93</b>
<b>Ours*</b>	<b><u>21.64</u></b>	<b><u>6.03</u></b>	<b><u>6.37</u></b>

Table 2. Comparison with state-of-the-art methods on HIC dataset [22].

Methods	PA-MPJPE	PA-MPVPE
METRO [28]	6.7	6.8
MeshGraphomer [9]	6.3	6.5
AMVUR [3]	6.2	6.1
HaMeR [17]	6.0	5.7
Zhou et al. [29]	5.8	6.1
<b>Ours</b>	<b>5.3</b>	<b>5.4</b>
<b>Ours*</b>	<b><u>5.1</u></b>	<b><u>5.2</u></b>

Table 3. Comparison with state-of-the-art methods on FreiHAND dataset [30].

each frame. It includes  $4 \times 32,560$  frames for training and 3,960 frames for evaluation and testing. **HO-3D** [1] focus on hand-object interactions, comprising 66,000 training images and 11,000 test images across 68 different sequences. **HIC** [22] offers a variety of hand-hand and object-hand interaction sequences, along with 3D ground truth meshes for both hands.

### 4.3. Evaluation metrics

We mainly adopt Mean Per Joint Position Error (MPJPE) and Mean Per Vertex Position Error (MPVPE) to measure the 3D errors (in millimeters) of the pose and shape of each estimated hand after aligning them using a root joint translation, and Mean Relative-Root Position Error (MRRPE) to measure the performance of relative positions (in millimeters) of two hands. Procrustes-aligned mean

per joint position error (PA-MPJPE) and Procrustes-aligned mean per vertex position error (PA-MPVPE) refer to the MPJPE and MPVPE after aligning the predicted hand results with the Ground Truth using Procrustes alignment, respectively. To better investigate the impact of incorporating additional 2D information on performance, we introduce MPJPE-XY, MPJPE-Z, MPVPE-XY, and MPVPE-Z in the ablation study. These metrics calculate the hand recovery error of MPJPE and MPVPE relative to the ground truth in the XY and Z dimensions, respectively.

### 4.4. Comparison with state-of-the-art methods

**Quantitative results in InterHand 2.6M datasets.** We conduct a comprehensive comparison of our method with recent state-of-the-art (SOTA) hand pose and shape estimation methods on the InterHand 2.6M test dataset, as presented in Table 1. The MRRPE metric effectively reflects the estimation performance of relative hand distances. Our method achieves the best performance on this metric with 21.60mm, surpassing InterWild, Ren et al., and 4DHands by 5.14mm, 7.38mm, and 2.98mm respectively. Our method also demonstrates consistent improvement in MPJPE and MPVPE, outperforming the current best method, 4DHands, by 2.13mm and 2.14mm respectively. Furthermore, we observe consistent performance gains in both the IH MPJPE/MPVPE and SH MPJPE/MPVPE metrics, highlighting the generalizability and robustness of our method for both single-hand and interacting hand estimation. Moreover, we have significantly surpassed the performance of Zuo et al. [31], which incorporates prior interactive features, demonstrating the superiority of our method.

**Quantitative results in HIC.** We present the results on the HIC dataset [22], which features in-the-wild cross-hand data, to evaluate performance in real-world scenarios. The training sets for these models don’t contain the HIC dataset. In Table 2, we compare these results with IntagHand, InterWild, and 4DHands, a state-of-the-art method specifi-

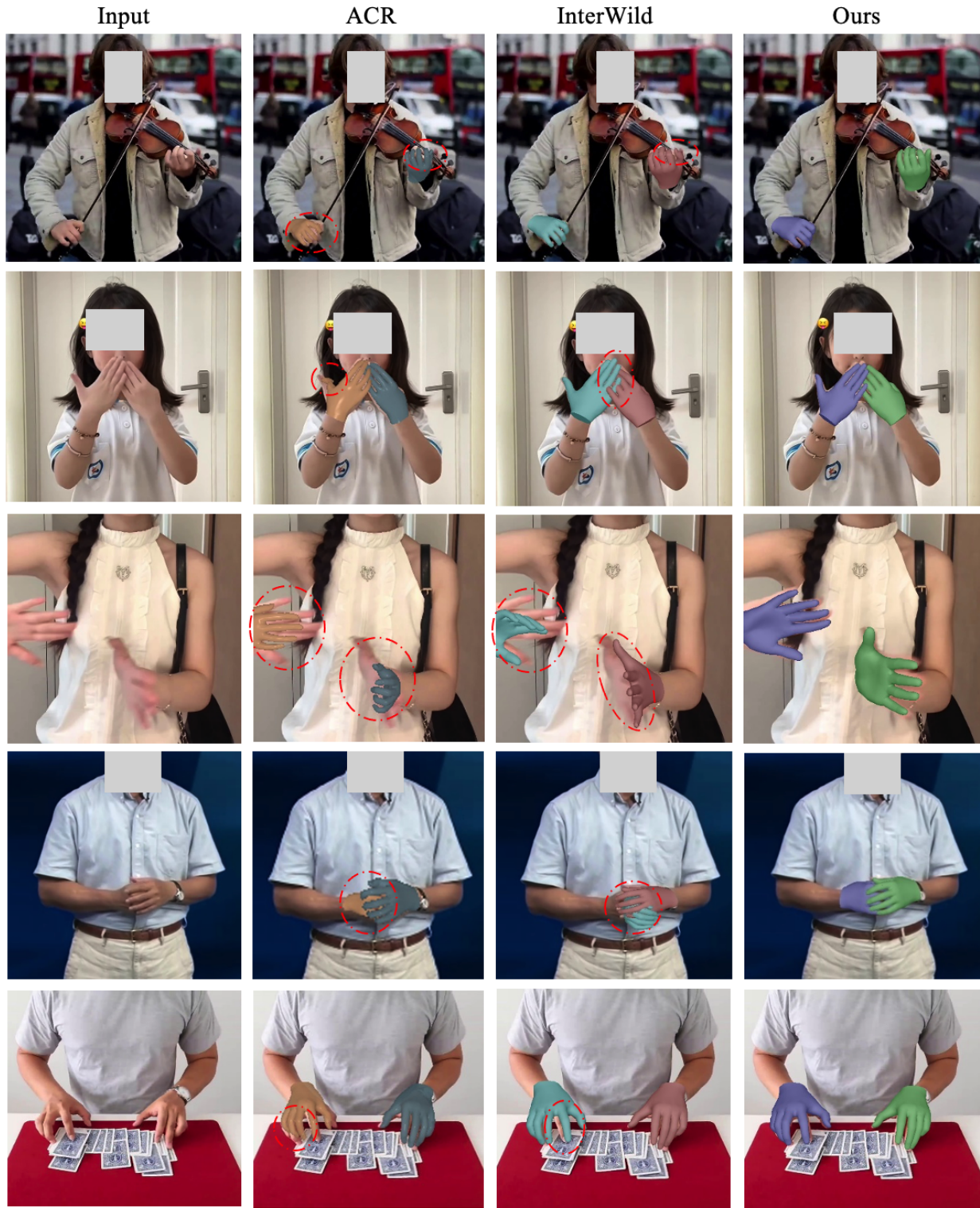


Figure 3. Qualitative results in real scenes. The images are all sourced from the internet. The red circle indicates distortion or inaccurate estimation.

Methods	MRRPE	MPJPE	MPVPE	MPJPE-XY	MPJPE-Z	MPVPE-XY	MPVPE-Z
Baseline	25.30	7.77	7.93	5.21	4.54	5.29	4.63
+ <b>2D Keypoints</b>	24.71	6.48	6.72	4.28	4.43	4.39	4.53
+ <b>Segmentation map</b>	24.52	6.19	6.34	4.21	4.40	4.33	4.50
+ <b>Depth map</b>	22.38	5.74	5.98	4.13	3.37	4.19	3.46
+ <b>Two-hand Diffusion</b>	<b>21.60</b>	<b>5.36</b>	<b>5.58</b>	<b>3.87</b>	<b>3.01</b>	<b>3.76</b>	<b>3.05</b>

Table 4. Ablation studies on InterHand2.6M [13].

cally designed for two-hand recovery in the wild. Our method outperformed 4Dhands and InterWild across multiple metrics without using foundation model inference. Specifically, it improved MRRPE by 3.02mm and 4.79mm, MPJPE by 2.65mm and 8.95mm, and MPVPE by 3.00mm and 8.80mm, respectively. These results highlight its superior stability on unseen data.

**Quantitative results with single-hand method on FreiHAND dataset.** We also compared our method with the latest state-of-the-art transformer-based single-hand recovery methods on the FreiHAND dataset [30]. In this comparison, our method omits the estimation of the relative translation between the two hands and the execution of diffusion for both hands. Table 3 reveals our method’s superiority over HaMer and Zhou et al. (without foundation models), with PA-MPJPE enhancements of 0.7mm and 0.5mm, and PA-MPVPE gains of 0.3mm and 0.7mm, respectively. This affirms our method’s efficacy in enhancing single-hand estimation through additional priors integration.

**Qualitative results.** We visually compare our method with open-sourced ACR and InterWild on real-world internet images, highlighting performance differences. As shown in Fig. 3, in the first row, both ACR and InterWild show misalignment issues. In the second row, ACR estimates relative hand distance but suffers from thumb distortion, while InterWild exhibits hand penetration. The third row features occlusion and blur, where ACR and InterWild fail to recover poses, but our method succeeds. In the fourth row, ACR incorrectly estimates the left hand, and InterWild shows hand penetration. Finally, in the last row, both ACR and InterWild produce misaligned estimations. Our method consistently achieves more accurate and stable results, demonstrating superior robustness in challenging scenarios.

#### 4.5. Ablation study

**Effectiveness of different prior inputs.** As shown in Table 4, we gradually added different types of information for fusion to observe their impact on performance. We observed that adding 2D keypoints and segmentation maps resulted in significant improvements in MPJPE and MPVPE, with the greatest reduction in the XY dimension estimation error. It is easy to understand that 2D keypoints and segmentation maps provide excellent XY dimension information cues. We can observe that 2D keypoints enhanced

performance more significantly than segmentation maps, as they offer detailed joint-level data, unlike the mere outlines provided by segmentation maps. Moreover, after fusing depth maps, we observed significant improvements in MPJPE/MPVPE-Z and MRRPE. Depth maps can clearly help the model better reason about the hierarchical relationships of the 3D hand.

**Effectiveness of using two-hand diffusion model.** Table 4 also demonstrates the impact of the two-hand diffusion model on hand recovery performance. We can see that after adding diffusion, MRRPE, MPJPE, and MPVPE all achieve improvements and with the same improvement trend in both the XY and Z dimensions. The two-hand diffusion model can effectively learn the reasonable two-hand interacting prior, which can help adjust the relative relationship between the hands to a more reasonable state.

## 5. Conclusion

In this paper, we propose a two-hand reconstruction method that integrates additional 2D reference information to improve hand alignment and depth recovery performance. Furthermore, when one hand is occluded by another (making the 2D reference information for the occluded hand unreliable), we introduce a two-hand diffusion model as an interacting prior to address the penetration issue. Extensive qualitative and quantitative experimental results demonstrate that our method significantly outperforms previous two-hand and single-hand reconstruction approaches.

**Limitation and Future Work:** Our method still faces challenges in handling extreme occlusions and motion blur in hand images, as the additional 2D information may become unreliable under such conditions. We believe that future integration of temporal processing could effectively alleviate this problem.

## References

- [1] Shreyas Hampali, Mahdi Rad, Markus Oberweger, and Vincent Lepetit. Honnotate: A method for 3d annotation of hand and object poses. In *Proceedings of the IEEE/CVF conference on computer vision and pattern recognition*, pages 3196–3206, 2020. 5, 6
- [2] Kaiming He, Xiangyu Zhang, Shaoqing Ren, and Jian Sun. Deep residual learning for image recognition. In *Proceed-*



- ings of the IEEE conference on computer vision and pattern recognition, pages 770–778, 2016. 5
- [3] Zheheng Jiang, Hossein Rahmani, Sue Black, and Bryan M Williams. A probabilistic attention model with occlusion-aware texture regression for 3d hand reconstruction from a single rgb image. In *Proceedings of the IEEE/CVF Conference on Computer Vision and Pattern Recognition*, pages 758–767, 2023. 3, 6
- [4] Sheng Jin, Lumin Xu, Jin Xu, Can Wang, Wentao Liu, Chen Qian, Wanli Ouyang, and Ping Luo. Whole-body human pose estimation in the wild. In *Computer Vision–ECCV 2020: 16th European Conference, Glasgow, UK, August 23–28, 2020, Proceedings, Part IX 16*, pages 196–214. Springer, 2020. 5
- [5] Rawal Khirodkar, Timur Bagautdinov, Julieta Martinez, Su Zhaoen, Austin James, Peter Selednik, Stuart Anderson, and Shunsuke Saito. Sapiens: Foundation for human vision models. *arXiv preprint arXiv:2408.12569*, 2024. 1, 5, 6
- [6] Jihyun Lee, Shunsuke Saito, Giljoo Nam, Minhyuk Sung, and Tae-Kyun Kim. Interhandgen: Two-hand interaction generation via cascaded reverse diffusion. In *Proceedings of the IEEE/CVF Conference on Computer Vision and Pattern Recognition*, pages 527–537, 2024. 3, 5
- [7] Mengcheng Li, Liang An, Hongwen Zhang, Lianpeng Wu, Feng Chen, Tao Yu, and Yebin Liu. Interacting attention graph for single image two-hand reconstruction. In *Proceedings of the IEEE/CVF Conference on Computer Vision and Pattern Recognition*, pages 2761–2770, 2022. 1, 3, 6
- [8] Dixuan Lin, Yuxiang Zhang, Mengcheng Li, Yebin Liu, Wei Jing, Qi Yan, Qianying Wang, and Hongwen Zhang. 4dhands: Reconstructing interactive hands in 4d with transformers. *arXiv preprint arXiv:2405.20330*, 2024. 1, 3, 5, 6
- [9] Kevin Lin, Lijuan Wang, and Zicheng Liu. Mesh graphormer. In *Proceedings of the IEEE/CVF international conference on computer vision*, pages 12939–12948, 2021. 1, 2, 6
- [10] Tsung-Yi Lin, Michael Maire, Serge Belongie, James Hays, Pietro Perona, Deva Ramanan, Piotr Dollár, and C Lawrence Zitnick. Microsoft coco: Common objects in context. In *Computer Vision–ECCV 2014: 13th European Conference, Zurich, Switzerland, September 6–12, 2014, Proceedings, Part V 13*, pages 740–755. Springer, 2014. 5
- [11] Chengqi Lyu, Wenwei Zhang, Haiyan Huang, Yue Zhou, Yudong Wang, Yanyi Liu, Shilong Zhang, and Kai Chen. Rtm-det: An empirical study of designing real-time object detectors. *arXiv preprint arXiv:2212.07784*, 2022. 5
- [12] Gyeongsik Moon. Bringing inputs to shared domains for 3d interacting hands recovery in the wild. In *Proceedings of the IEEE/CVF Conference on Computer Vision and Pattern Recognition*, pages 17028–17037, 2023. 1, 3, 4, 5, 6
- [13] Gyeongsik Moon, Shou-I Yu, He Wen, Takaaki Shiratori, and Kyoung Mu Lee. Interhand2. 6m: A dataset and baseline for 3d interacting hand pose estimation from a single rgb image. In *Computer Vision–ECCV 2020: 16th European Conference, Glasgow, UK, August 23–28, 2020, Proceedings, Part XX 16*, pages 548–564. Springer, 2020. 1, 5, 6, 8
- [14] Gyeongsik Moon, Shunsuke Saito, Weipeng Xu, Rohan Joshi, Julia Buffalini, Harley Bellan, Nicholas Rosen, Jesse Richardson, Mallorie Mize, Philippe De Bree, et al. A dataset of relighted 3d interacting hands. *Advances in Neural Information Processing Systems*, 36, 2024. 1, 5
- [15] Lea Müller, Vickie Ye, Georgios Pavlakos, Michael Black, and Angjoo Kanazawa. Generative proxemics: A prior for 3d social interaction from images. In *Proceedings of the IEEE/CVF Conference on Computer Vision and Pattern Recognition*, pages 9687–9697, 2024. 1
- [16] Adam Paszke, Sam Gross, Francisco Massa, Adam Lerer, James Bradbury, Gregory Chanan, Trevor Killeen, Zeming Lin, Natalia Gimelshein, Luca Antiga, et al. Pytorch: An imperative style, high-performance deep learning library. *Advances in neural information processing systems*, 32, 2019. 5
- [17] Georgios Pavlakos, Dandan Shan, Ilija Radosavovic, Angjoo Kanazawa, David Fouhey, and Jitendra Malik. Reconstructing hands in 3d with transformers. In *Proceedings of the IEEE/CVF Conference on Computer Vision and Pattern Recognition*, pages 9826–9836, 2024. 1, 3, 6
- [18] Pengfei Ren, Chao Wen, Xiaozheng Zheng, Zhou Xue, Haifeng Sun, Qi Qi, Jingyu Wang, and Jianxin Liao. Decoupled iterative refinement framework for interacting hands reconstruction from a single rgb image. In *Proceedings of the IEEE/CVF International Conference on Computer Vision*, pages 8014–8025, 2023. 6
- [19] Javier Romero, Dimitrios Tzionas, and Michael J Black. Embodied hands: modeling and capturing hands and bodies together. *ACM Transactions on Graphics (TOG)*, 36(6):1–17, 2017. 2, 3
- [20] Soyong Shin, Juyong Kim, Eni Halilaj, and Michael J Black. Wham: Reconstructing world-grounded humans with accurate 3d motion. In *Proceedings of the IEEE/CVF Conference on Computer Vision and Pattern Recognition*, pages 2070–2080, 2024. 1, 3
- [21] Guy Tevet, Sigal Raab, Brian Gordon, Yonatan Shafir, Daniel Cohen-Or, and Amit H Bermano. Human motion diffusion model. *arXiv preprint arXiv:2209.14916*, 2022. 5
- [22] Dimitrios Tzionas, Luca Ballan, Abhilash Srikantha, Pablo Aponte, Marc Pollefeys, and Juergen Gall. Capturing hands in action using discriminative salient points and physics simulation. *International Journal of Computer Vision*, 118:172–193, 2016. 5, 6
- [23] Yufu Wang, Ziyun Wang, Lingjie Liu, and Kostas Daniilidis. Tram: Global trajectory and motion of 3d humans from in-the-wild videos. In *European Conference on Computer Vision*, pages 467–487. Springer, 2024. 1
- [24] Yuliang Xiu, Jinlong Yang, Xu Cao, Dimitrios Tzionas, and Michael J Black. Econ: Explicit clothed humans optimized via normal integration. In *Proceedings of the IEEE/CVF conference on computer vision and pattern recognition*, pages 512–523, 2023. 3
- [25] Zhengdi Yu, Shaoli Huang, Chen Fang, Toby P Breckon, and Jue Wang. Acr: Attention collaboration-based regressor for arbitrary two-hand reconstruction. In *Proceedings of the IEEE/CVF Conference on Computer Vision and Pattern Recognition*, pages 12955–12964, 2023. 1, 3, 4, 6

- [26] Baowen Zhang, Yangang Wang, Xiaoming Deng, Yinda Zhang, Ping Tan, Cuixia Ma, and Hongan Wang. Interacting two-hand 3d pose and shape reconstruction from single color image. In *Proceedings of the IEEE/CVF international conference on computer vision*, pages 11354–11363, 2021. 6
- [27] Lvmin Zhang, Anyi Rao, and Maneesh Agrawala. Adding conditional control to text-to-image diffusion models. In *Proceedings of the IEEE/CVF International Conference on Computer Vision*, pages 3836–3847, 2023. 3
- [28] Xiong Zhang, Qiang Li, Hong Mo, Wenbo Zhang, and Wen Zheng. End-to-end hand mesh recovery from a monocular rgb image. In *Proceedings of the IEEE/CVF International Conference on Computer Vision*, pages 2354–2364, 2019. 2, 6
- [29] Zhishan Zhou, Shihao Zhou, Zhi Lv, Minqiang Zou, Yao Tang, and Jiajun Liang. A simple baseline for efficient hand mesh reconstruction. In *Proceedings of the IEEE/CVF Conference on Computer Vision and Pattern Recognition*, pages 1367–1376, 2024. 3, 6
- [30] Christian Zimmermann, Duygu Ceylan, Jimei Yang, Bryan Russell, Max Argus, and Thomas Brox. Freihand: A dataset for markerless capture of hand pose and shape from single rgb images. In *Proceedings of the IEEE/CVF International Conference on Computer Vision*, pages 813–822, 2019. 5, 6, 8
- [31] Binghui Zuo, Zimeng Zhao, Wenqian Sun, Wei Xie, Zhou Xue, and Yangang Wang. Reconstructing interacting hands with interaction prior from monocular images. In *Proceedings of the IEEE/CVF international conference on computer vision*, pages 9054–9064, 2023. 3, 5, 6